

## Article

# Determination of the Kinetic Parameters of Thermal Degradation and Hydrodemetallization of a Mixture of the Heavy Fraction of Low-Temperature Coal Tar and Coal Shale

Murzabek Baikenov <sup>1,\*</sup>, Dariya Izbastanova <sup>1</sup>, Akmaral Sarsenbekova <sup>1</sup> , Nazerke Balpanova <sup>1</sup>, Almas Tusipkhan <sup>1,\*</sup>, Zukhra Khalikova <sup>1</sup>, Nazym Rakhimzhanova <sup>1</sup>, Elena Kochegina <sup>1</sup>, Balzhan Tulebaeva <sup>2</sup> and Gulzhan Taurbaeva <sup>2</sup>

<sup>1</sup> Department of Chemical Technologies and Petrochemicals, Faculty of Chemistry, Karaganda Buketov University, Karaganda 100028, Kazakhstan; dom\_dariya@mail.ru (D.I.); chem\_akmaral@mail.ru (A.S.); nazerke\_90@mail.ru (N.B.); khalikova1979@mail.ru (Z.K.); raximzhanova82@mail.ru (N.R.); kochegina79@mail.ru (E.K.)

<sup>2</sup> Department of Natural and Scientific Disciplines, Baitursynov Kostanay Regional University, Kostanay 110000, Kazakhstan; nissantule@bk.ru (B.T.); taurbaeva\_kspi@mail.ru (G.T.)

\* Correspondence: thearticle@bk.ru or baikenov.murzabek@list.ru (M.B.); almas\_kz\_22@mail.ru (A.T.)

**Abstract:** The laws of thermal degradation of the mixture of the heavy fraction of low-temperature coal tar and coal shale were investigated using dynamic thermogravimetry. The kinetic characteristics of the process were determined using various methods, including the Ozawa–Flynn–Wall, Friedman, non-parametric kinetics and Šesták–Berggren methods. It is shown that coal shale initiated changes in the kinetic parameters and decomposition rate of the heavy fraction of coal tar. It was found that a 13% content of coal shale in the mixture led to the maximum rate of weight loss of the heavy fraction of coal tar. A hydrodemetallization kinetic model of the mixture of the heavy fraction of low-temperature coal tar and coal shale is proposed. The kinetic parameters of the hydrodemetallization process were determined; in addition, the rate constants at various temperatures were estimated. The study shows that the distribution of trace elements in the hydrogenate from the initial mixture and in the hydrogenate from the solid residue was characterized by relatively low values of reaction rate constants. The maximum microelement distribution rate was achieved in the hydrogenate solid residue. Energy indicators of activation processes indicated that hydrodemetallization at low temperatures is advantageous from an energy point of view.

**Keywords:** demetallization; hydrodemetallization; germanium; cobalt; vanadium; molybdenum; coal tar; coal shale; thermogravimetric; hydrodemetallization kinetic



**Citation:** Baikenov, M.; Izbastanova, D.; Sarsenbekova, A.; Balpanova, N.; Tusipkhan, A.; Khalikova, Z.; Rakhimzhanova, N.; Kochegina, E.; Tulebaeva, B.; Taurbaeva, G. Determination of the Kinetic Parameters of Thermal Degradation and Hydrodemetallization of a Mixture of the Heavy Fraction of Low-Temperature Coal Tar and Coal Shale. *Energies* **2024**, *17*, 1766. <https://doi.org/10.3390/en17071766>

Academic Editor: Shu Tao

Received: 2 March 2024

Revised: 31 March 2024

Accepted: 3 April 2024

Published: 8 April 2024



**Copyright:** © 2024 by the authors. Licensee MDPI, Basel, Switzerland. This article is an open access article distributed under the terms and conditions of the Creative Commons Attribution (CC BY) license (<https://creativecommons.org/licenses/by/4.0/>).

## 1. Introduction

Solid- and heavy-hydrocarbon feedstocks such as coal, shale, heavy petroleum residue and coal tar are a promising source of important elements including germanium, gallium, vanadium, nickel and rare earths (yttrium, scandium, silver and others) [1–5]. Eighty-four elements of the periodic system were found in solid- and heavy-hydrocarbon materials, mainly in the form of trace elements. Heavy metals contained in heavy oil and oil residues preclude the recovery of catalyst activity during the processing of heavy-hydrocarbon materials [6].

In most cases, trace elements are present in solid- and heavy-hydrocarbon feedstocks at a level greater than or equal to that in ore feedstocks [4]. Therefore, special attention is paid to demetallization technologies that allow such raw materials to be included in processing procedures. The analysis of literature sources showed [6,7] that there are various methods for the demetallization of heavy-oil raw materials (heavy oil, oil residues, tar, oil sludge, etc.); however, the accumulation of microelements into the solid phase from coal tar and coal shale has not been sufficiently investigated [4]. It should be noted that coal tar resulting

from the coking of coal contains the largest amount of valuable trace elements. Oil shales, in turn, differ from coals by containing from 8 to 20% of organic substances. They also contain valuable trace elements such as germanium, lanthanum, vanadium, molybdenum and others, the content of which is comparable to that in industrial ores [4,8–11].

Our objective was to integrate rare elements from sources such as coal shale, coal tar and the high-temperature coal tar fraction into a solid product composition. The use of coal shale and the high-temperature fraction of coal tar provides high value to our research.

The demetallization by destructive conversion of a mixture of coal tar and coal shale involves processes that should provide the highest degree of conversion of the mixture and the lowest amount of non-converted residue in which the metals of the raw material are concentrated. In this regard, the development and implementation of technologies for processing the mixture create real prerequisites for the achievement of the high-inversion complex processing of the heavy fraction of coal tar and coal shale, with metals concentrated in a solid product. Using combustible coal shale in the processing of the heavy fraction of coal tar, it is possible to obtain a raw material enriched in metals.

Due to the complex composition of the mixture of coal tar heavy fraction and coal shale, detailed data on the decomposition rate of their organic components at different temperatures are required to develop efficient and selective processing methods. The investigation of the demetallization mechanism of solid-hydrocarbon feedstock, such as a mixture of coal resin fractions and coal shale, is of great interest.

The study of the demetallization process includes two main stages: the first is a thermogravimetric analysis, and the second is the creation of a kinetic model for the hydrodemetallization of coal resin and shale. We previously investigated the thermal decomposition of primary coal tar by heterogeneous catalysts using the thermogravimetric analysis method. This method allowed us to determine mass loss and kinetic parameters and to carry out the process of thermal decomposition of the resin at different heating rates [12,13].

The purpose of this work was to study the kinetics of thermal degradation using the thermogravimetry method and perform a kinetic analysis of the hydrodemetallization of a mixture of low-temperature coal tar and coal shale.

## 2. Materials and Methods

The heavy fraction of low-temperature coal tar obtained by the fractionation of low-temperature coal tar at atmospheric pressure was selected for the study.

Two mixtures containing 5% coal shale and the heavy fraction of low-temperature coal tar and 13% coal shale and the heavy fraction low-temperature coal tar were prepared. The ratio of coal tar heavy fraction to coal shale (with 5 and 13% of coal shale) was selected on the basis of literature sources [14,15].

The original coal shale was shredded in a shear mill, and particles smaller than 0.1 and 0.1 mm in size were screened out using a *SieveShaker OBRK-SA* (Cangzhou oubeiruike instrument and Equipment CO., LTD., Cangzhou, China, 2022) device and stored in polyethylene bags.

The IR spectra of the mixture of the heavy fraction of coal tar and coal shale were recorded on an FSM1201 IR-Fourier spectrometer, with the following specifications: transmission mode, range 400–4000  $\text{cm}^{-1}$ , resolution 8.0  $\text{cm}^{-1}$ , 20 scans, comparison spectrum—general, KBr beam splitter with coating based on Ge.

Thermal decomposition of the mixture was carried out using a LabsysEvoTG-DTA/DSC (Setaram, Caluire, France, 2012r) derivatograph in corundum crucibles in the temperature range from 30 to 600 °C in an argon stream (the flow rates of the protective and purge gas were 20 and 50 mL per minute, respectively). The measurement results were processed using the OriginLab software package and the Python Anaconda3 distribution, version 3.11.15. A reference standard— $\text{CaCO}_3$ , calcium carbonate—was used to control the thermal degradation of the mixture.

The kinetics of thermal degradation of the mixture was determined by the Ozawa–Flynn–Wall, Friedman, non-parametric kinetics and Šesták–Berggren methods.

At the starting time,  $\alpha$  is equal to 0, and at the end of the process,  $\alpha = 1$ . A mathematical model of the reactions can be represented by a differential equation with the initial condition corresponding to the value of  $\alpha$  of reagent A at the start of the reaction ( $t = 0$ ):

$$\frac{d\alpha_A(t)}{dt} = -k\alpha_A(t)^n \quad (1)$$

$$\alpha_A(0) = \alpha_{A_0}$$

The determination of kinetic parameters using the TG curve is based on the formal equation of kinetics:

$$\frac{d\alpha}{dt} - \beta \frac{d\alpha}{dT} - k(T)f(\alpha) - A \exp\left(-\frac{E_\alpha}{RT}\right)f(\alpha) \quad (2)$$

where  $\alpha$  is the degree of completion of the process,  $t$  is time,  $T$  is temperature,  $\beta$  is the heating rate (K/min),  $f(\alpha)$  is the kinetic model,  $k(T)$  is a rate constant that depends on the temperature according to the Arrhenius equation, with the parameters  $A$  (pre-exponential factor) and  $E_a$ —(activation energy), and  $R$  is the universal gas constant.

The Friedman method [16] is the most common and frequently used isoconversion method. This method is based on the following equation [17]:

$$\ln\left(-\frac{dx}{dt}\right) = \ln A + \ln f(x) - \frac{E}{RT} \quad (3)$$

Using Equation (2) as a basis, Friedman proposes to take the logarithm of the reaction rate  $d\alpha/dt$  as a function of temperature at a given conversion rate. The resulting Friedman kinetic model for the  $n$ -order reaction is as follows:

$$\ln\left(\beta \frac{d\alpha}{dT_\alpha}\right) = \ln\{A_\alpha f(\alpha)\} - \frac{E_\alpha}{RT} \quad (4)$$

The dependence of the conversion rate expressed as the  $d\alpha/dt$  logarithm of the inverse of the temperature,  $1/T$ , is described by a straight line, the inclination angle of which is  $m = E_a/R$ .

Mathematically, the Ozawa–Flynn–Wall method is represented as follows:

$$\log \beta = -1.052 \frac{E_\alpha}{RT_\alpha} + 5.3305 + \ln\left\{\frac{R}{AE_\alpha} \int_0^1 \frac{d\alpha}{f(\alpha)}\right\} \quad (5)$$

The logarithm of the  $\ln(\beta)$  ratio depending on the inverse of the temperature,  $1/T$ , defines a straight line with an angular coefficient  $m = -1.052 E_a/R$ .

The kinetics analysis of the hydrodemetallization process of the mixture was carried out according to a formalized scheme (Figure 1), where  $C_1$  is the content of trace elements in the mixture of coal shale and the heavy fraction of low-temperature tar with a boiling point above 300 °C,  $C_2$  is the content of trace elements in the hydrogenate, and  $C_3$  is the content of trace elements in the solid residue, in %.

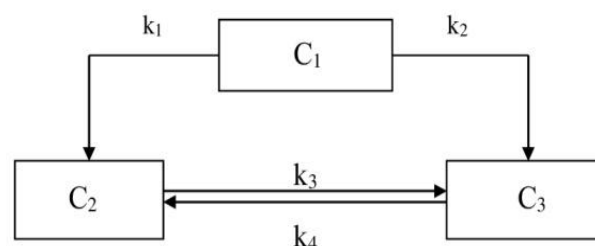


**Figure 1.** Formalized mechanism of the hydrodemetallization kinetics of the mixture of the heavy fraction of coal tar and coal shale.

The rate constants were calculated on the basis of experimental data, duration of the experiments from 15 to 75 min and temperature of 380–420 °C. In accordance with the proposed scheme, a kinetic model of the mixture hydrodemetallization process was compiled, which has the following form:

$$\frac{dc_1}{d\tau} = -(k_1 + k_2)C_1 \quad (6)$$

$$\frac{dc_2}{d\tau} = k_1C_1 - k_3C_2 + k_4C_3 \quad (7)$$

$$\frac{dc_3}{d\tau} = k_2C_1 - k_3C_2 + k_4C_3 \quad (8)$$

where  $C_1$ – $C_3$  indicate the trace element content at a point in time  $\tau$ . The system of differential equations was solved using the Davidon–Fletcher–Powell method and the random search method.

The hydrodemetallization kinetics of the mixture was determined in a high-pressure reactor with a stirring device and a volume of 0.5 L. The initial hydrogen pressure was 4 MPa, the weight of the mixture charge was 4 g, the duration of the analysis was from 15 to 75 min, the heating temperature was from 380 to 420 °C.

The concentration of trace elements in the initial mixture, hydrogenate and solid residue was determined using an atomic emission spectral method based on electric arc burning of the sample by employing a diffraction spectrograph 8 equipped with a multi-channel atomic emission spectrum analyzer (MAES).

### 3. Results and Discussion

The heavy fraction of coal tar with boiling point above 300 °C had the following elemental composition in wt%:  $H^{daf}$ —8.0,  $C^{daf}$ —62.0,  $S^{daf}$ —1.0,  $N^{daf}$ —2.0,  $O^{daf}$ —39.0. The elemental composition of coal shale, in wt%, was the following:  $H^{daf}$ —7.79,  $C^{daf}$ —63.08,  $S^{daf}$ —4.68,  $N^{daf}$ —1.74,  $O^{daf}$ —22.77,  $W^a$ —3.17,  $A^a$ —64.58.

The elemental composition of the mixture of 13% coal shale and the heavy fraction of coal tar with boiling point above 300 °C, in wt%, was the following:  $H^{daf}$ —6.58,  $C^{daf}$ —69.69,  $S^{daf}$ —0.37,  $N^{daf}$ —1.16,  $O^{daf}$ —22.21,  $A^a$ —11.2.

The studied samples, including the mixture of the heavy fraction of low-temperature coal tar and coal shale (5% and 13%), made it possible to evaluate the effect of the added coal shale amount on the thermal degradation of the mixture. Carrying out the thermal destruction of the heavy fraction of low-temperature coal tar including 13% and 5% of coal shale under various temperature conditions allowed us to predict the likelihood of accumulation of trace elements in the solid residue. As a result of our research, using isoconversion models, we identified the main kinetic characteristics of the decomposition process of the heavy fraction of low-temperature coal tar including 13% and 5% of coal shale. The results of the study showed the practical value of this method. The curves of the thermogravimetric analysis and decomposition rate obtained are presented in Figure 2.

As shown in Figure 2, samples of the heavy fraction of coal tar + 13% and 5% of coal shale in a nitrogen atmosphere began to decompose at ~100 °C. Then, till ~150 °C, a slight decomposition of the sample, with evaporation of the internal and hygroscopic moisture, was observed. Observing the thermogravimetric curves of the heavy fraction of coal tar with 13% and 5% of shale (Figure 2a,b), we concluded that the coal tar with the addition of 13% of coal shale reached the maximum decomposition rate of the sample, which is reflected by the peak in the DTG curve (Figure 2c), at a temperature of about 323 °C. In this case, the total weight loss of the sample during heating was approximately 78.21% (Figure 2a). A similar behavior was observed for the heavy fraction of coal tar with the addition of 5% of coal shale: the maximum decomposition rate of the sample, as seen from the peak in the DTG curve, occurred at a temperature of about 350 °C, and the total mass loss of the second copolymer when heated was about 77.07% (Figure 2b). The degradation process of both samples was substantially complete at a temperature of about 600 °C.

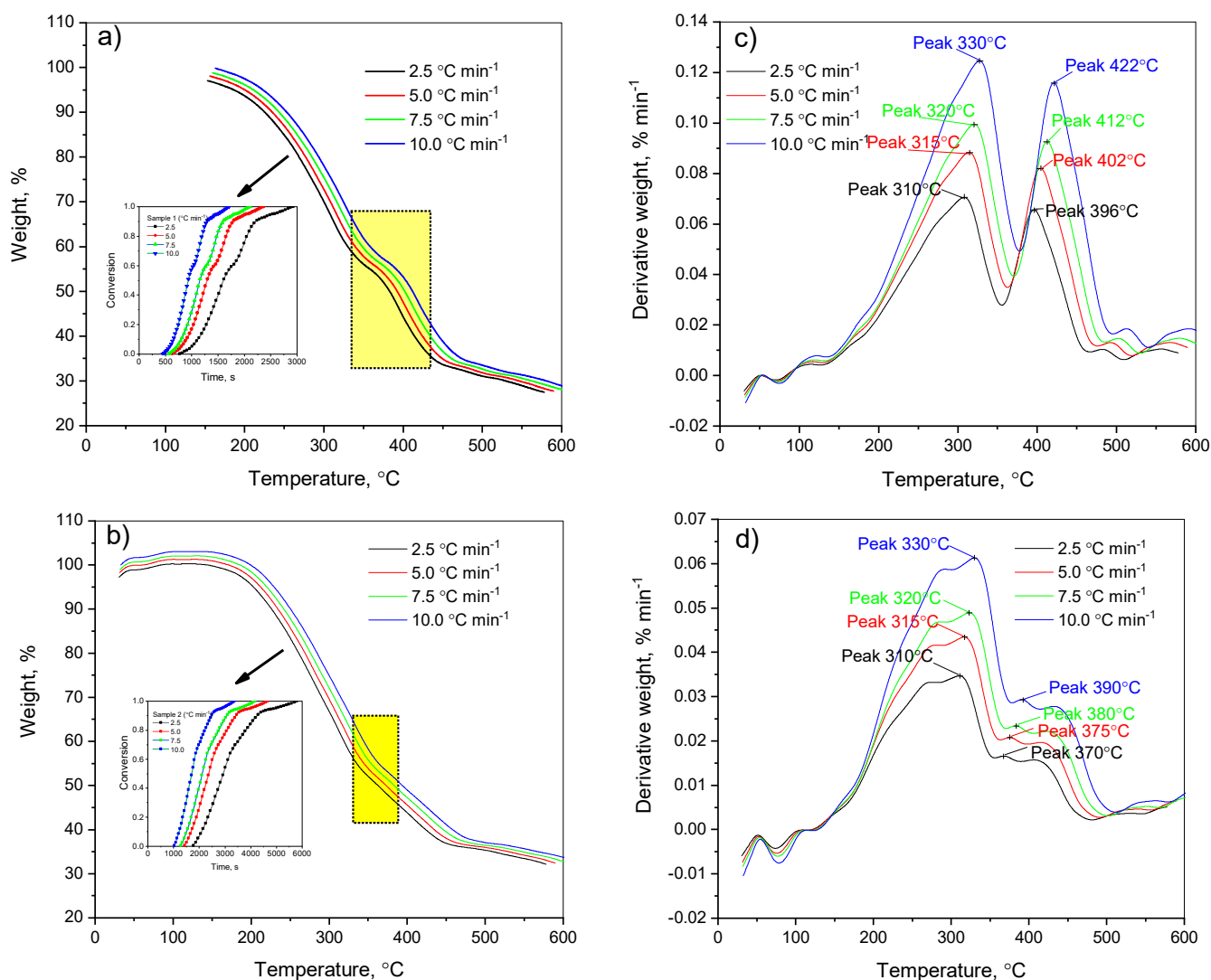


**Figure 2.** Dependence of sample mass on temperature (a,b) and rate of mass change (c,d) for (a) heavy fraction of coal tar + 13% of coal shale and (b) heavy fraction of coal tar + 5% of coal shale in a nitrogen atmosphere.

Some volatile products present in the heavy coal tar fraction containing 13% and 5% of coal shale could be determined from a specific strong infrared absorption peak, indicating that the gas phase components of the pyrolysis products were mainly  $\text{CO}_2$  ( $2356\text{ cm}^{-1}$ ) and molecules containing  $\text{CH}_2$  aliphatic groups. The IR spectra confirmed that the absorption of the  $\text{CH}_2$  aliphatic group in the region of valence ( $2918, 2849\text{ cm}^{-1}$ ) and deformation ( $613, 999, 1454\text{ cm}^{-1}$ ) vibrations signified a high content of hydrogenated cycles. In the IR decomposition spectrum (Figure 3) of the heavy fraction of coal tar containing 13% of coal shale at a temperature from 350 to  $600\text{ }^\circ\text{C}$ , the intensity of the valence oscillation band of  $\text{CO}_2$  groups ( $2360\text{ cm}^{-1}$ ) increased.

An analysis of the literature on the thermal degradation of the heavy fraction of coal tar with the addition of coal shale [18–22] showed that the available information on thermogravimetric and IR spectroscopic analyses was incomplete, which prevented us from conducting a comparative analysis of the results obtained.

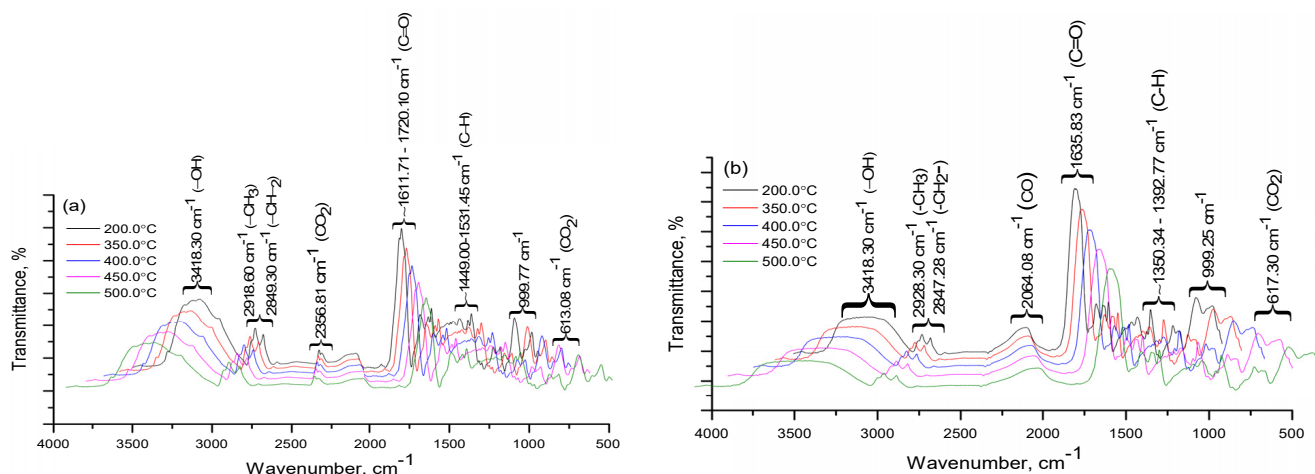


**Figure 3.** Degradation product IR spectra recorded from 0 to 600 °C for (a) heavy fraction of coal tar + 13% of coal shale and (b) heavy fraction of coal tar + 5% of coal shale.

Reactions involving solids, such as the thermal decomposition of coal, belong to a special class of topological processes that are characterized by the localization of the reaction zone at the interface between the solid reactant and the reaction product. Under these conditions, the concept of concentration of a reactant substance loses its meaning, and it is more convenient to use the parameter  $\alpha$ , which denotes the proportion of reacted substances at a point in time.

The key fact that attracted the attention of scientists [14–16,23] during these studies is that the kinetic characteristics calculated based on isothermal data are not directly related to the chosen model, while kinetic values based on non-isothermal methods show an inverse relationship.

The method of calculating non-isothermal kinetics was proposed simultaneously in the works of Ozawa [23] and Flynn and Wall [24]. The advantage of this method is the ability to determine the activation energy without knowing the functions  $f(\alpha)$  and  $g(\alpha)$ , but this is only true under the assumption that the reaction is one-step.

The use of the above methods made it possible to graphically determine the thermodynamic parameters of the process of thermal decomposition of the heavy fraction of coal tar including 13% and 5% of coal shale at different heating rates and conversion levels (Figure 4, Table 1).

The analysis showed that the values of the kinetic parameters of the overall reaction obtained by calculation (Table 1 and Figure 4) were lower than those of each single parallel reaction, namely,  $\bar{E} = 86.32$  kJ/mol,  $\alpha = 0.1$  and  $\bar{E} = 87.52$  kJ/mol,  $\alpha = 1.0$ , that is, the parameters of the gross process were of a purely formal nature.

**Table 1.** Activation energy values of the heavy fraction of low-temperature coal tar + 13% and 5% of coal shale at different heating rates in a nitrogen atmosphere.

Sample	$\bar{A}, s^{-1}$	$\bar{E}_{FR}, kJmol^{-1}$	$\bar{A}, s^{-1}$	$\bar{E}_{FWO}, kJmol^{-1}$
Heavy fraction of coal resin + 13% coal shale	$3.30 \times 10^5$	83.54	15.71	84.25
Heavy fraction of coal resin + 5% coal shale	$3.46 \times 10^4$	83.73	0.62	84.69



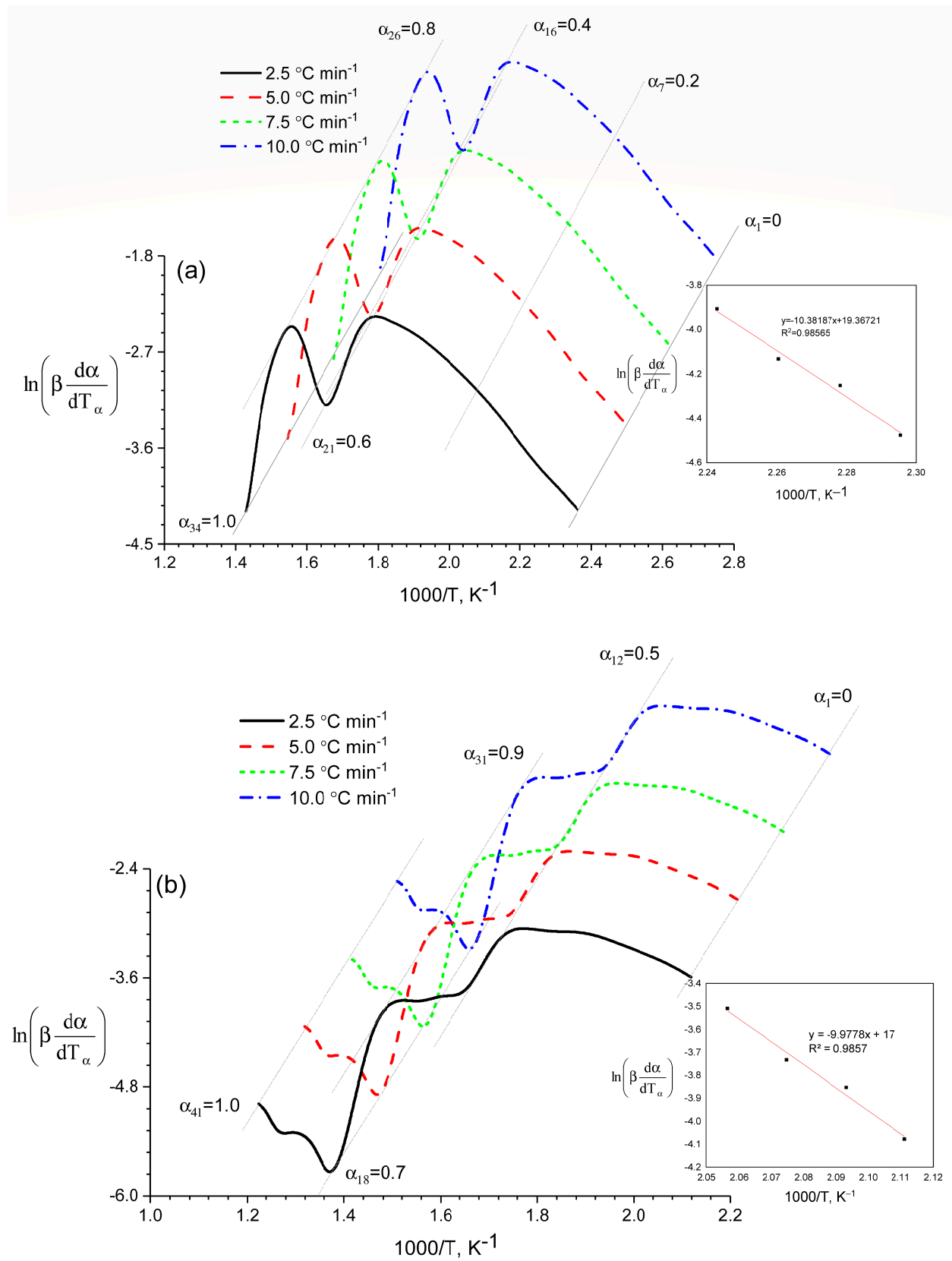


**Figure 4.** Schematic representation of the Friedman differential method. (a) heavy fraction of coal tar + 13% of coal shale and (b) heavy fraction of coal tar + 5% of coal shale.

Both groups of methods described above are based on the use of the Arrhenius equation. It should be noted that in the Arrhenius equation

$$k = k_0 e^{-E_a/RT} \quad (9)$$

the rate constant  $k$  and temperature  $T$  play the role of dependent and independent variables, and  $k_0$  and  $E_a$  are the parameters to be estimated.

The partial derivatives of  $k$  with respect to the other parameters are equal to:

$$\frac{\partial k}{\partial k_0} = e^{-E/RT} = \frac{k}{k_0} \quad (10)$$

$$\frac{\partial k}{\partial E} = -\frac{k_0}{RT} e^{-E/RT} = -\frac{k}{RT} \quad (11)$$

The observed triplet (which is a term often used to describe one set of  $A$ ,  $E_a$  and  $f(\alpha)$  or  $g(\alpha)$  values) depends on the ratio of the rate constants of the chemical process. But it should be borne in mind that this equation describes only the part of the S-shaped curve lying after the inflection point. In other words, Equation (9) is a special case of the more general kinetic equation  $\frac{d\alpha}{dt} = \varphi(t)f(\alpha)$ .

One of the methods that well describes the course of a reaction that occurs with an increase in the reaction rate is the informal kinetics method (IKM). The main distinguishing feature of the informal kinetics method is that it allows for determining formal kinetic parameters when processing a certain set of values ( $d\alpha/dt$ ,  $T$  and  $\alpha$ ).

It is necessary to consider in more detail the mathematical side of the nonparametric kinetics method. The nonparametric kinetics method [25] is based on constructing a matrix containing information on  $k(T)$  and  $f(\alpha)$ .

This matrix can generally be represented in the form of a singular value decomposition algorithm,  $M = U \cdot \Sigma \cdot V^T$  [25–28]. Below, the kinetic matrix (IKM) method is reported, where the reaction rate can be expressed as the product of two independent functions [18],  $k(T) = [\Sigma_1 v_1, \Sigma_1 v_2, \dots, \Sigma_1 v_j]$  and  $f(\alpha) = [u_1, u_2, \dots, u_i]$ .

The information matrix is equal to:

$$M = \{m_{ij}\} = \begin{Bmatrix} r(a_1, T_1) & r(a_1, T_2) & \dots & r(a_1, T_j) \\ r(a_2, T_1) & r(a_2, T_2) & \dots & r(a_2, T_j) \\ \dots & \dots & \dots & \dots \\ r(a_i, T_1) & r(a_i, T_2) & \dots & r(a_i, T_j) \end{Bmatrix} \quad (12)$$

The experimental reaction rate data were obtained using Equation (5) (Table 2) and are presented in a 3D system (Figure 5).

The choice of  $f(\alpha)$  was carried out using the Šesták–Berggren method, often called the Prout–Tompkins (P-T) equation [26,27], by selecting the most appropriate model in the coordinates  $(d\alpha/dt) - \alpha$  at different heating rates ( $\beta$ ).  $f(\alpha) = \alpha^m(1 - \alpha)^n$  was used as the function  $f(\alpha)$ . The parameters  $m$  and  $n$  affect the shape and position of the maximum of the curve  $(d\alpha/dt)$  (Figure 6). The results of the kinetic analysis are shown in Figure 6 and Table 2.

**Table 2.** Values of the kinetic parameters of the thermal decomposition process at various ratios of heavy fraction of coal tar to shale.

Sample	$\bar{E}_{NPK}$ , kJ mol <sup>−1</sup>	$\bar{A}$ , s <sup>−1</sup>	Šesták–Berggren		$\bar{E}_{Sh-B}$ , kJ mol <sup>−1</sup>	$\bar{A}$ , s <sup>−1</sup>
			$\alpha^m(1 - \alpha)^n$			
			m	n		
Heavy fraction of coal tar + 13% coal shale	83.63	3.30·10 <sup>5</sup>	0.23	0.55	83.63	8.42·10 <sup>5</sup>
Heavy fraction of coal tar + 5% coal shale	85.80	3.48·10 <sup>4</sup>	0.41	0.76	85.58	1.17·10 <sup>5</sup>



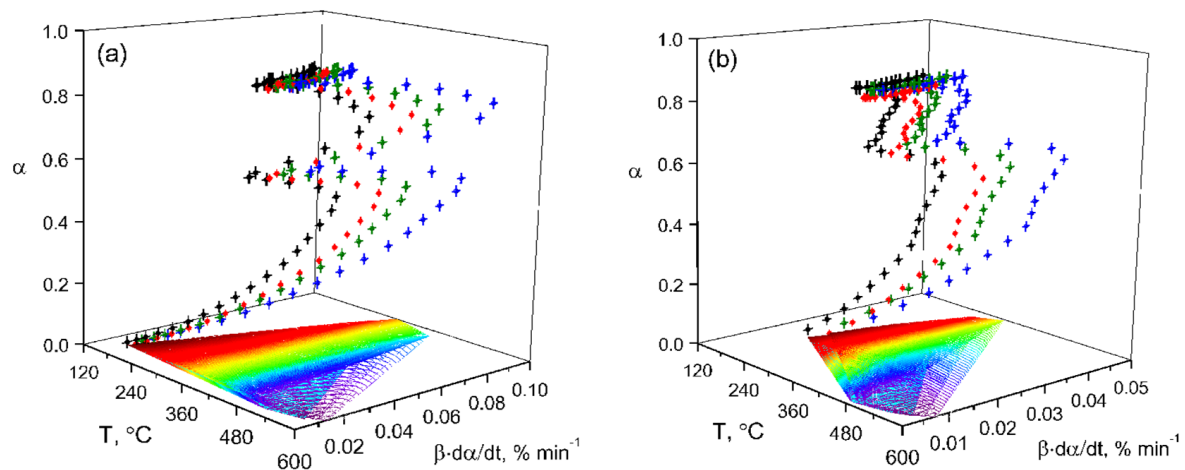


**Figure 5.** Experimental data in 3D space. Samples consisting of (a) 13% of shale + heavy fraction of coal tar and (b) 5% of shale + heavy fraction of coal tar.

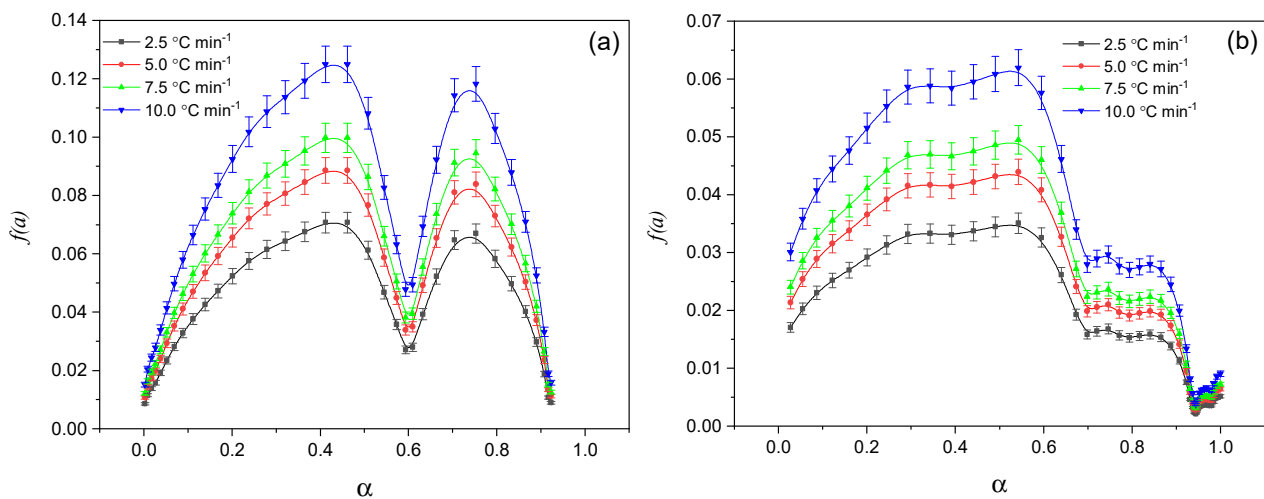


**Figure 6.** Graphical method for solving the Šesták–Berggren model. Samples consisting of (a) 13% of shale + heavy fraction of coal tar and (b) 5% of shale + heavy fraction of coal tar.

For the data in Figure 6a, the equation  $f(\alpha) = \alpha^{0.23}(1 - \alpha)^{0.55}$  was obtained, while, for the data in Figure 6b, the equation  $f(\alpha) = \alpha^{0.41}(1 - \alpha)^{0.76}$  was derived. As can be seen in Figure 6, the exponents  $m$  and  $n$  (where  $>1$ ) are concave downwards, which corresponds to a retarding type of kinetics. This indicates that in the processes described by these equations, the maximum activation energy was achieved at the initial stage and gradually decreased with the increasing degree of decomposition.

The expression of the kinetics of thermal destruction made it possible to establish the influence of temperature on the reaction rate constant. It was established that the parameter  $k$  obeys the Arrhenius law (Figure 7).

A review of the results showed that the  $E$ - $\alpha$  curves (Figure 8) from each individual method (FR, NPK and SH-B) had the same shape. According to the data reported in Table 2 and Figure 8a, we obtained the values  $\alpha = 0.1$  and  $\alpha = 1.0$  with  $\bar{E}_{max}(0.1) = 86.32$  kJ/mol and  $\bar{E}_{max}(1.0) = 87.52$  kJ/mol. For the mixture of 5% of coal shale + the heavy fraction of coal tar, one point corresponding to the maximum value of the activation energy was obtained in the decomposition zone of the heavy fraction of coal tar. The degree of conversion in this case was 1.0, and the activation energy was 93.86 kJ/mol (Figure 8b).

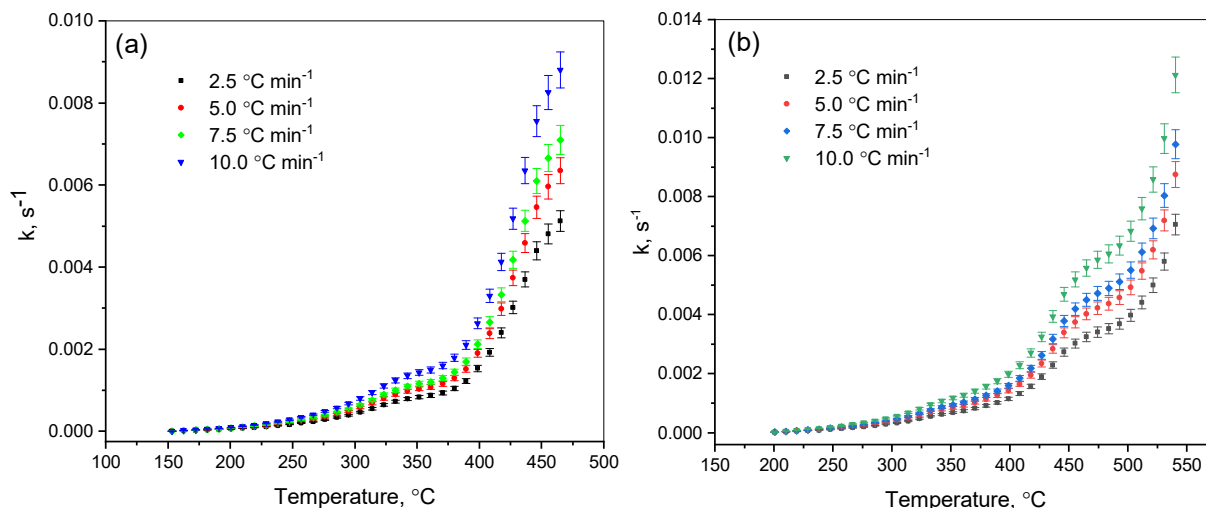


**Figure 7.** Dependence of the reaction rate constant on temperature. Samples containing (a) 13% shale + heavy fraction of coal tar and (b) 5% shale + heavy fraction of coal tar.

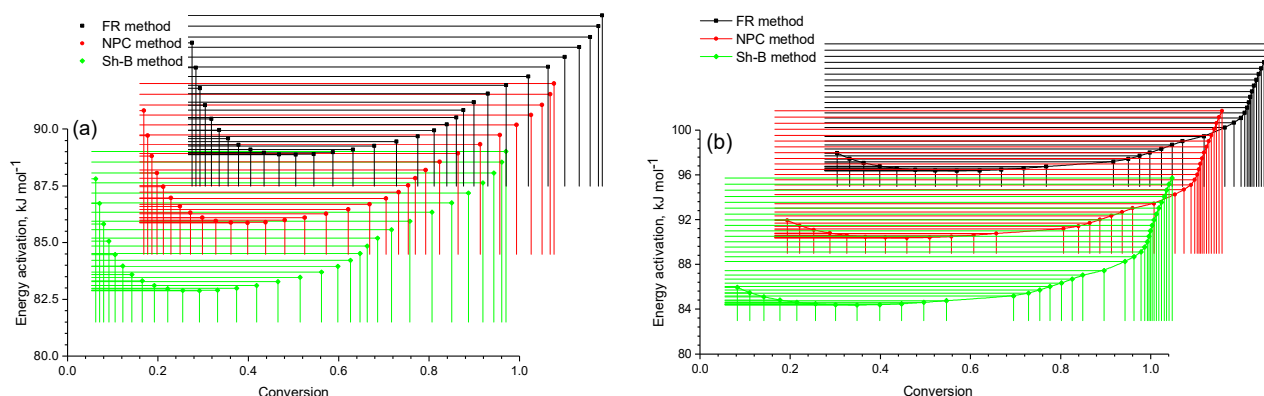


**Figure 8.** Activation energy indicators (E) determined using the Friedman (FR), nonparametric kinetics (NPK) and Shestak–Berggren (SH-B) methods. Samples containing (a) 13% coal shale + heavy fraction of coal tar and (b) 5% coal shale + heavy fraction of coal tar.

Thus, based on the results obtained, it can be concluded that the thermal destruction process of the mixture with 13% of coal shale was carried out under milder conditions than that of the mixture with 5% of coal shale. This was proved by the obtained data on the dependence of the sample mass on the temperature and the rate of change in the mass of the mixture.

For the further study of the hydrometallization kinetics of the mixture of the heavy fraction of low-temperature tar and coal shale, the mixture consisting of the heavy fraction of low-temperature tar and 13% of coal shale was used.

To determine the kinetic parameters, the hydrometallization of the mixture was carried out at temperatures from 380 to 420 °C for a duration of 15 to 75 min. The concentration of trace elements in the mixture components depending on the temperature and holding time is presented in Table 3.

The kinetics of the hydrometallization process of the mixture of coal shale and tar fraction with boiling point higher than 300 °C was established using the Davidon–Fletcher–Powell method under a low initial hydrogen pressure. The formalized scheme includes reactions leading to the formation of products that contain trace elements (Figure 1). In the proposed scheme,  $[C_i]$  is the content of trace elements at the  $i$  time. The system of differential equations was solved using a random search method. The velocity constants were optimized to minimize the sum of the squares of the differences between the experimental

and the calculated values of the weight fractions of the hydrodemetallization products from the mixture.

**Table 3.** Content of hydrodemetallization products in the components of the coal shale and tar fraction mixture with boiling point higher than 300 °C.

No.	Conditions $\tau$ , min	Content of Trace Elements, wt%			
		In the Initial Mixture	In the Hydrogenate	In the Solid Residue	Degree of the Mixture Demetallization, % of the Mixture
			Temperature 380 °C		
1	15	52.1	19.0	28.9	47.9
2	30	45.4	17.5	37.1	54.6
3	45	40.1	14.9	45.0	59.9
4	60	36.5	13.3	50.2	63.5
5	75	33.0	11.3	55.7	67.0
			Temperature 400 °C		
6	15	50.7	18.2	31.1	56.8
7	30	45.0	16.8	38.2	66.0
8	45	39.0	14.2	46.8	71.6
9	60	36.0	12.0	52.0	79.6
10	75	30.0	10.4	59.6	87.8
			Temperature 420 °C		
11	15	48.7	16.0	35.3	66.4
12	30	43.7	15.0	41.3	74.9
13	45	37.9	12.7	49.4	80.8
14	60	35.0	8.1	56.9	90.3
15	75	29.1	6.4	64.5	99.1

The reaction rate constants of the components were calculated according to the formalized scheme. The rate constants  $k_1$ ,  $k_2$ ,  $k_3$  and  $k_4$  characterized the reaction rate of the hydrodemetallization of the mixture and the distribution of trace elements in its components. The rate constants were calculated based on the experimental data reported in Table 3.

The velocity constants were optimized on the condition of the minimum sum of the squared deviations between experimental and calculated values of the weight fractions of the hydrodemetallization products of the mixture. The values obtained for the direct rate constants  $k_1$ ,  $k_2$ ,  $k_3$  of the hydrodemetallization process showed the rapid progress of direct hydrodemetallization reactions in the mixture. The inverse rate constant  $k_3$ , indicating the content of trace elements in the hydrogenate, suggested a low speed.

The reaction rate constants of the accumulation of trace elements in the three components were calculated. The calculated rate constants of the hydrodemetallization reactions in the mixture are presented in Table 4.

In the process of creating the kinetic model of the mixture hydrodemetallization, it was necessary to estimate the rate constants at different temperatures. The calculation of these constants was carried out on the basis of the experimental data on the hydrodemetallization of the mixture, presented in Table 3. Table 4 shows the calculated rate constants of the mixture hydrodemetallization process.

From the data presented in Table 4, it follows that the rate constant increased as the temperature increased. At the same time, the distribution of trace elements in the hydrogenate from the initial mixture ( $k_1$ ) and in the hydrogenate from the solid residue ( $k_4$ ) showed relatively low values of reaction rate constants. The maximum microelement distribution rate was achieved in the solid residue from the hydrogenate ( $k_3$ ).

The activation energy was calculated using the Arrhenius equation. The results showed the concentration of trace elements in the hydrogenate and solid residue, as well as the calculated activation energy values, which were 30.7 kJ/mol, 32.0 kJ/mol, 67.47 kJ/mol and 91.3 kJ/mol. The data obtained indicate that the distribution of trace elements in the

hydrogenate and solid product was the least energetically hindered stage. The activation energy of the distribution of trace elements from the hydrogenate to the solid residue and back was three times higher than the activation energy for the C<sub>3</sub>-to-C<sub>2</sub> step, amounting to 91.3 kJ/mol. From this, it can be concluded that in order to ensure the selectivity of the hydrodemetallization process aimed at distributing trace elements into a solid residue and reducing their content in the hydrogenate, the increase in the process temperature should be limited.

**Table 4.** Rate constants of hydrodemetallization reactions in the mixture of coal shale and coal tar heavy fraction with boiling point above 300 °C.

Temperature	Rate Constants, min <sup>−1</sup>			
	k <sub>1</sub>	k <sub>2</sub>	k <sub>3</sub>	k <sub>4</sub>
380	0.0029	0.00396	0.0295	0.0033
400	0.0036	0.00465	0.048	0.00687
420	0.00405	0.0056	0.08	0.005
	Activation energy, kJ/mol			
E	30.7	32.1	91.3	67.5
	Correlation coefficient, R			
R	0.99	0.98	0.99	0.99

The results of the analysis of the metal content in the solid product (presented in Table 3) confirmed that the process of hydrodemetallization of the mixture was also influenced by sorption processes. When, besides the temperature, the contact time increased from 15 to 75 min, the content of trace elements in the solid product increased from 28.9 to 64.5 wt%.

The data obtained show that the process of demetallization of the heavy fraction of low-temperature coal tar during hydrogenation with coal shale is a complex of chemical interactions. These include interactions of heavy-fraction metal-containing fragments with organic and mineral parts of coal shale, as well as the possible adsorption of metals in the heavy-fraction tar on the mineral surface of coal shale. Probably, organomineral components are able to catalyze the process of destruction of high-molecular-weight compounds in the heavy fraction of coal tar. This will facilitate their more intensive conversion to light liquid and gaseous products and also promote the formation of densification products. Such densification products will bind the metals in the heavy fraction of coal tar and in coal shale.

The described technology of hydrodemetallization of the mixture of the heavy fraction coal tar and coal shale can lead to the production of solid products with a significant content of rare metals.

#### 4. Conclusions

On the basis of the obtained data reflecting the dependence of the mass of the samples on temperature and the rate of change in the mass of the mixture, it can be concluded that during the thermal destruction process, a higher rate of decomposition of the heavy fraction of coal tar was observed when 13% of coal shale was added than when the mixture with 5% of coal shale was used.

The study of the thermal decomposition kinetics of the heavy fraction of coal tar with the addition of 13% and 5% of coal shale made it possible to determine the kinetic parameters of the decomposition reaction under non-isothermal conditions. These parameters made it possible to ensure the preservation of the kinetic triplet and a more adequate description of the process. The obtained energy profiles by various analytical and calculation methods showed that the decomposition of the organic mass of the heavy fraction of low-temperature coal tar containing 13% and 5% of coal shale under thermal exposure began with reactions characterized by lower activation energy values ( $E_a$ ) compared to those of reactions occurring in the absence of coal shale. It was found that the process of

thermal degradation of the mixture continued with an uneven increase in activation energy along the reaction path, indicating the multi-step nature of the process. The kinetic results obtained made it possible to predict the destruction of the mixture, consisting of a heavy fraction of coal tar and 13% and 5% of coal shale, under thermal conditions.

Various aspects of the hydrodemetallization reaction were analyzed, and the dependence of the concentration of trace elements in the mixture derivatives on the conditions of heat treatment and hydrodemetallization of the mixture was revealed. Using the kinetic model, the kinetic parameters of the hydrodemetallization process, such as activation energy and rate constant, were calculated. The values of the activation energy processes indicated the energy benefit of hydrodemetallization at low temperatures.

Hydrodemetallization of the heavy fraction of coal tar and coal shale with a high ash content (65%) is a promising strategy with wide application in the field of resource saving. This means that such process can solve the economic problems associated with the processing of oil and the extraction of rare metals from alternative sources of raw materials, as well as improve the environmental situation in areas of utilization of solid and heavy hydrocarbons.

**Author Contributions:** Conceptualization, M.B.; methodology, M.B.; software, A.T, N.B., B.T. and G.T.; validation, M.B., A.T., Z.K. and E.K.; formal analysis, M.B., D.I. and Z.K.; investigation, M.B., N.B., A.S. and D.I.; resources, A.T., G.T. and B.T.; data curation, Z.K., N.R. and E.K.; writing—original draft preparation, M.B. and A.T.; writing—review and editing, M.B., A.T. and N.B.; visualization, E.K., D.I., A.S. and N.R.; supervision, B.T., G.T., D.I. and A.S.; project administration, A.T. and M.B. All authors have read and agreed to the published version of the manuscript.

**Funding:** This research and APC was funded by the Ministry of Science and Higher Education of the Republic of Kazakhstan (registration No. 0123PK00217), state grant No. AP19679059.

**Data Availability Statement:** The original contributions presented in the study are included in the article, further inquiries can be directed to the corresponding authors.

**Conflicts of Interest:** The authors declare no conflicts of interest.

## References

1. Seredin, V.V.; Dai, S. Coal deposits as potential alternative sources for lanthanides and yttrium. *Int. J. Coal Geol.* **2012**, *94*, 67–93. [\[CrossRef\]](#)
2. Dai, S.; Finkelman, R.B. Coal as a promising source of critical elements: Progress and future prospects. *Int. J. Coal Geol.* **2018**, *186*, 155–164. [\[CrossRef\]](#)
3. Sorokin, A.P.; Agiev, O.A.; Dugin, S.V.; Popova, A.A. Metal carrier of brown coals of the Raichikhinsky field (Amur region, Far East): Conditions for accumulation of distribution, prospects for development (overview). *Solid Fuel Chem.* **2023**, *1*, 13–31.
4. Lapidus, A.L.; Khudyakov, D.S.; Beilina, N.Y.; Trukhina, M.A.; Kozlov, A.M.; Zhagfarov, F. Solid combustible fossils as a source of trace elements. *Solid Fuel Chem.* **2022**, *1*, 3–18. [\[CrossRef\]](#)
5. Kobotaeva, N.S.; Skorokhodova, T.S. Integrated use of adsorbents and ultrasonic exposure in the process of metal removal from fuel oil. *Pet. Chem.* **2023**, *3*, 380–390. [\[CrossRef\]](#)
6. Magomedov, R.N.; Popova, A.Z.; Kadiev, H.M.; Khadzhiev, S.N. Status and Prospects for Demetallization of Heavy Crude Oil (Overview). *Pet. Chem.* **2015**, *55*, 267–290. [\[CrossRef\]](#)
7. Khojiev, S.N.; Shpirt, M.Y. *Trace Elements in Oils and Products of Their Processing*; Science: Moscow, Russia, 2012.
8. Spirt, M.Y.; Nukenov, D.N.; Punanova, S.A.; Visaliev, M.Y. Principles for Obtaining Valuable Metal Compounds from Combustible Minerals. *Solid Fuel Chem.* **2013**, *47*, 71–82. [\[CrossRef\]](#)
9. Tashmukhambetova, Z.K.; Kairbekov, Z.K.; Aubakirov, E.A. Hydrogenation processing of carbon-containing wastes in a mixture with oil shale from the Kenderlyk deposit. *Solid Fuel Chem.* **2016**, *50*, 220–225. [\[CrossRef\]](#)
10. Kadiev, K.M.; Gyl'maliev, A.M.; Zekel', L.A.; Kadieva, M.K. Hydrofining of oil shale pyrolysis tar in the presence of ultradispersed catalysts. *Solid Fuel Chem.* **2018**, *52*, 336–342. [\[CrossRef\]](#)
11. Maloletnev, A.S.; Kairbekov, Z.K.; Smagulova, N.T. Refining of Coal Tar by Hydrogenation in the Presence of Nanoheterogeneous Nickel Sulfide Catalyst. *Coke Chem.* **2020**, *63*, 253–256. [\[CrossRef\]](#)
12. Tyanakh, S.; Tusipkhan, A.; Gyl'maliev, M.; Yun, M.F.; Baikenova, G.G.; Kainenov, D.A.; Khalitova, A.I.; Baikenov, M.I. Kinetic study of thermal decomposition of primary coal tar in the presence of catalysts with nickel, cobalt and iron oxides supported on the microsilicate. *Solid Fuel Chem.* **2022**, *1*, 19–27. [\[CrossRef\]](#)
13. Balpanova, N.; Baikenov, M. Thermal Degradation Kinetics of Vacuum Residues in the Presence of Chrysotile Supported Ni-Ti Catalyst. *Catalysts* **2023**, *13*, 1361. [\[CrossRef\]](#)

14. Gorlova, S.E.; Moroz, I.V.; Gyulmisaryan, T.G.; Berengarten, M.G.; Gorlov, E.G. Thermal cracking of fuel oil with addition of combustible shales. *Solid Fuel Chem.* **2002**, *36*, 29–40.
15. Gorlova, S.E.; Moroz, I.V.; Gyulmisaryan, T.G.; Berengarten, M.G.; Gorlov, E.G. Thermal cracking of petroleum mazut with oil shale additives. *Solid Fuel Chem.* **2002**, *4*, 33–47.
16. Friedman, H.L. New methods for evaluating kinetic parameters from thermal analysis data. *J. Polym. Sci. Part B* **1969**, *7*, 41–46. [\[CrossRef\]](#)
17. Maryandyshev, P.A. Thermal Energy Fundamentals of Using Wood Biofuel. Doctoral Dissertation, Northern (Arctic) Federal University named after M.V. Lomonosov, Arkhangelsk, Russia, 2019.
18. Strizhakov, D.A.; Yusevich, A.I.; Yurachka, V.V.; Kadiev, K.M.; Agabekov, V.E.; Hadzhiev, S.N. Kinetics of thermolysis of a mixture of tar and pine sawdust. *Petrochemistry* **2016**, *56*, 475–482.
19. Fetisova, O.Y. Kinetic study of the stage of thermal decomposition of various coals of Mongolia. *Solid Fuel Chem.* **2021**, *1*, 3–10.
20. Shin, S.; Im, S.I.; Nho, N.S.; Lee, K.B. Kinetic analysis using thermogravimetric analysis for nonisothermal pyrolysis of vacuum residue. *J. Therm. Anal. Calorim.* **2016**, *126*, 933–941. [\[CrossRef\]](#)
21. Xu, Y.; Zhang, Y.; Wang, Y.; Zhang, G.; Chen, L. Thermogravimetric study of the kinetics and characteristics of the pyrolysis of lignite. *React. Kinet. Mech. Catal.* **2013**, *110*, 225–235. [\[CrossRef\]](#)
22. Maryandyshev, P.A.; Chernov, A.A.; Popova, E.I.; Lyubov, V.K. Study of the process of thermal decomposition and combustion of coal, wood fuel and hydrolysis lignin by thermal analysis method. *Solid Fuel Chem.* **2016**, *50*, 167–176. [\[CrossRef\]](#)
23. Ozawa, T. New method of analyzing thermogravimetric data. *Bull. Chem. Soc. Jpn.* **1965**, *38*, 1881–1886. [\[CrossRef\]](#)
24. Flynn, J.H.; Wall, L.A. A quick, direct method for the determination of activation energy from thermogravimetric data. *J. Polym. Sci. Part B Polym. Lett.* **1966**, *4*, 323–328. [\[CrossRef\]](#)
25. Sarsenbekova, A.Z.; Figurinene, I.V.; Khalitova, A.I. Comparative kinetic analysis of thermal destruction of hydrogel on the base of polymethylvinyl maleic acid ester linked with polypropylene glycol. *Bull. L.N. Gumilyov Eurasian Natl. Univ.* **2018**, *22*, 43–52.
26. Serra, R.; Nomen, R.; Sempere, J. The non-parametric kinetics a new method for the kinetic study of thermoanalytical data. *J. Therm. Anal. Calorim.* **1998**, *52*, 933–943. [\[CrossRef\]](#)
27. Šesták, J.; Kratochvíl, J. Rational approach to thermodynamic processes and constitutive equations in isothermal and non-isothermal kinetics. *J. Therm. Anal.* **1973**, *5*, 193–201. [\[CrossRef\]](#)
28. Šesták, J. Errors of kinetic data obtained from thermogravimetric curves at increasing temperature. *Talanta* **1966**, *13*, 567–579. [\[CrossRef\]](#)

**Disclaimer/Publisher's Note:** The statements, opinions and data contained in all publications are solely those of the individual author(s) and contributor(s) and not of MDPI and/or the editor(s). MDPI and/or the editor(s) disclaim responsibility for any injury to people or property resulting from any ideas, methods, instructions or products referred to in the content.